Three-nucleon short range correlations studies in inclusive scattering for $0.8 < Q^2 < 2.8$ (GeV/c)^2

J. Arrington (co-spokesperson), P. Solvignon (co-spokesperson, contact), D. F. Geesaman, K. Hafidi, R. Holt, P. Reimer
Argonne National Laboratory, Argonne, IL 60439

D. Higinbotham (co-spokesperson), D. Gaskell, D. Meekins, V. Sulkosky, S.A. Wood
Thomas Jefferson National Accelerator Facility, Newport News, VA 23606

D. B. Day (co-spokesperson), H. Baghdasaryan, D. Crabb, N. Fomin, O. Rondon, K. Slifer
University of Virginia, Charlottesville, VA, 22901

M. Sargsian
Florida International University, Miami, FL 33199

W. Bertozzi, S. Gilad, J. Huang, B. Moffit, P. Monaghan, N. Muangma, A. Puckett, N. Sparveris, X. Zhan
Massachusetts Institute of Technology, Cambridge, MA 02139

M. Strikman
Penn State University, University Park, PA 16802

E. Piasetzky, I. Pomerantz, G. Ron, R. Shneor
Tel Aviv University, Tel Aviv, 69978 Israel

and

The Hall A Collaboration

Abstract

We propose to perform a precision test of scaling in the region dominated by scattering from three-nucleon short range correlations (3N-SRC) in Hall A. If scaling in this region is valid, then one can use the ratio of scattering from heavier nuclei to ^{3}He as a measure of the relative contribution of 3N-SRC in heavier nuclei. The kinematics are chosen to emphasize the $x > 2.2$ region using an incident beam energy of 3.6 GeV, and the Hall A High Resolution Spectrometers in their standard configurations at several scattering angles from 15° to 29°. This measurement will provide more detailed information on the x and Q^2 dependence of the ratios for $x > 2.2$, which will allow us to verify scaling for $x > 2.2$, and thus confirm the dominance of 3N-SRC in this region and better extract the relative contribution of 2N- and 3N-SRCs in nuclei. Six nuclear targets will be used: ^{2}H, ^{3}He, ^{4}He, ^{12}C, ^{40}Ca and ^{48}Ca. By using calcium isotopes, we can have a first look at the isospin dependence of 2N- and 3N-SRC. The proposed experiment requires 12 days of beam time, including calibration, overhead, and background measurements, and uses only the HRS spectrometers with standard detector configurations.

I. MOTIVATIONS

While the structure of nuclei is relatively well described in terms of the nuclear shell model, measurements of the spectroscopic factors in (e,e'p) and other transfer reactions show a significant missing strength, on the scale of 30–40% of the nucleons. Short range correlations (SRCs) provide the largest depletion of shell model strength. The short range repulsive core of the N–N interaction yields a significant probability of a hard interaction between nucleons in the dense medium of a heavy nucleus. This leads to a dramatic increase in the number of extremely high-momentum nucleons ($k > k_F$) in the nucleus.

While single nucleon knockout reactions allow us to look at the shell model contributions, it is much more difficult to probe the high-momentum nucleons generated by correlations, as the cross section in this region has large contributions from other processes such as final-state interactions and meson-exchange currents. Inclusive electron scattering can be used to probe these high-momentum nucleons, providing cleaner measurements that complement the more detailed measurements possible in coincidence reactions.

Scattering from a proton is kinematically limited to values of Bjorken-x at or below one, with elastic scattering at $x = 1$. For a nucleus, $x \leq M_A/M_p \approx A$, but quasielastic scattering from a single nucleon occurs mainly near $x = 1$. The motion of the nucleon in the nucleus broadens the quasielastic (QE) peak, but for momenta at or below the Fermi momenta, k_F, there is little strength from QE scattering above $x = 1.3$. Above this region, the cross section is dominated by scattering from the high-momentum nucleons generated by short range correlations, and thus we can select kinematics that isolate scattering from these SRCs.

If we assume that the two-nucleon SRC involve only the two interacting nucleons and neglect their motion in the nucleus and any isospin dependence, the distribution of high-momentum nucleons coming from 2N-SRCs should be identical in all nuclei. The high-momentum tail in a heavy nucleus should then look similar to the high-momentum tail in deuterium, scaled up by the number of 2N-SRCs. This is the dominant contribution to the scattering up to $x = 2$, as the probability to have a multi-nucleon configuration generating high momentum nucleons is much smaller than the probability to have a two-nucleon configuration. For $x > 2$, the contribution from a stationary 2N-SRC vanishes and the scattering should be dominated by contributions from 3N-SRCs.

Using this basic picture, Frankfurt and Strikman [1, 2] showed that the cross section for $x \gtrsim 1.3$ is a sum of contributions from 2N, 3N,... correlations,

$$\begin{aligned}\sigma_A(x,Q^2) &= \sum_{j=2}^{A} \frac{A}{j} a_j(A)\sigma_j(x,Q^2) \\ &= \frac{A}{2}a_2(A)\sigma_2(x,Q^2) + \frac{A}{3}a_3(A)\sigma_3(x,Q^2) + ...,\end{aligned}$$

where σ_j is the cross section for scattering from a j-nucleon correlation and the constants $a_j(A)$ are proportional to the probability of finding a nucleon in a j-nucleon correlation which should fall rapidly with j as nuclei are dilute. Taking $a_j(A) = 1$ for $A = j$, i.e. defining $a_2(A)$ to be probability of finding a 2N-SRC in nucleus A relative to deuterium, the cross section σ_j reduces to the cross section for scattering from a nucleus with $A = j$, e.g. for $A = 2$, $\sigma_{eD}(x,Q^2) = a_2(A)\sigma_2(x,Q^2) = \sigma_2(x,Q^2)$, with $\sigma_j(x,Q^2) = 0$ for $x > j$.

In the region where 2N-SRCs dominate, the SRC model predicts scaling of the cross section ratio:

$$(2/A)\sigma_A(x,Q^2)/\sigma_D(x,Q^2) = a_j(A)/a_j(D) = a_j(A), \tag{1}$$

where the factor $(2/A)$ yields the ratio of cross sections per nucleon. Thus, for all values of x and Q^2 where the scattering is dominated by 2N-SRCs, the ratio of the cross section from a heavy nucleus to deuterium (or in fact the ratio of any two nuclei) should be independent of x and Q^2, and be a direct measure of the relative number of 2N-SRCs in the nuclei. While this neglects the effects of FSI, it has been argued [3] that in these small-sized SRCs, only the FSI between the nucleons within the correlation matter, and that these FSI should be identical as long as the nature of the correlations is identical for all nuclei, as assumed in the SRC model. Similar scaling should be observed in the ratio $A/^3He$ in the region where scattering from 3N-SRCs dominates.

The main assumptions in the SRC model are the isospin independence, and the assumption that the total momentum of the nucleons is zero, and thus the SRC is at rest with respect to the rest of the nucleus. We will return to the isospin dependence in Sec. III, although it is worth mentioning that while the simple SRC model assumes isospin independence, it is sufficient that the correlations are dominated by a single isospin configuration. The main effect of the small motion of the correlation in the nucleus is that it allows strength from a j-nucleon correlation to contribute to the scattering for values of x slightly larger than j. Because of this, 2N-SRCs can contribute for x values slightly larger than 2, and thus the region where 3N-SRCs are expected to dominate is $2.3 \lesssim x < 3$, rather than $2 < x < 3$.

While most experiments have compared to ^{2}H when examining 2N-SRCs and ^{3}He for 3N-SRCs, it is also useful to extract ratios of heavier nuclei to ^{4}He. This will allow a first look at $x > 3$, where 4N-SRCs are expected to dominate, and where we do not yet have any information on the onset of scaling. In addition, scaling for the 3N-SRC dominated region should be somewhat better than in the ratio to ^{3}He, as the 3N-SRC in ^{4}He has some motion which will partially cancel the effect of the 3N-SRC motion in the heavier nuclei. Finally, there is no issue with the assumption of isospin-independence for the ratios of ^{12}C or ^{40}Ca to ^{4}He.

This scaling behavior for 2N-SRCs was first observed in SLAC data [2, 4], and more recently in Hall C and Hall B at Jefferson Lab [5, 6]. The newest results from CLAS provided the first direct evidence for such scaling in the 3N-SRC region, as shown in Figure 1.

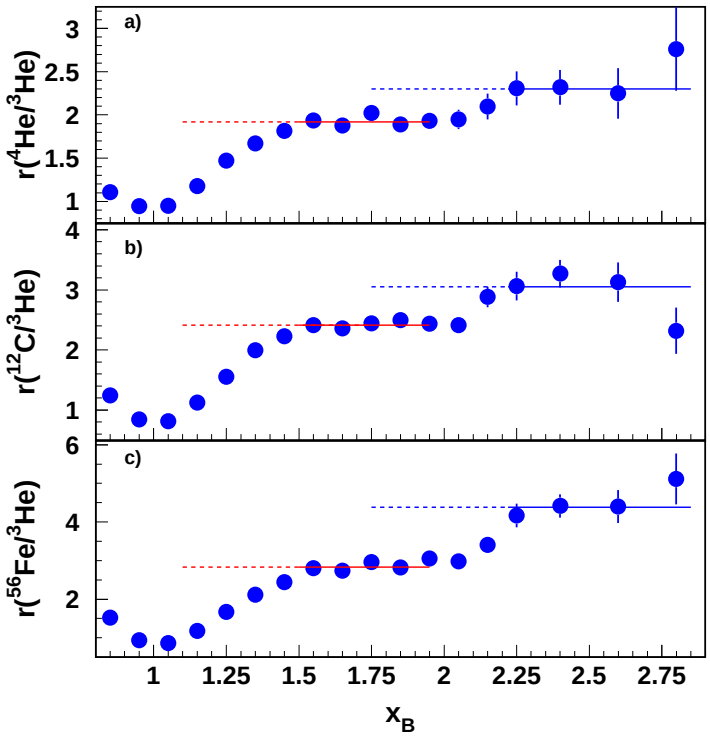

FIG. 1: 2N and 3N correlations from recent JLab Hall B data [6]. See text for definition of $r(\mathrm{A}/^3\mathrm{He})$.

Because these are ratios to ^{3}He, which is not an isoscalar nucleus, a correction has to be applied for the difference between σ_p and σ_n. Thus, the ratio plotted is not the cross section ratio, $R(\mathrm{A},^3\mathrm{He})=3\sigma_A/A\sigma_{^3He}$, but instead:

$$r(\mathrm{A},^3\mathrm{He}) = \mathrm{K}_3(\sigma_\mathrm{n},\sigma_\mathrm{p})\mathrm{R}(\mathrm{A},^3\mathrm{He}), \tag{2}$$

with $K_3(\sigma_n,\sigma_p) = \mathrm{A}(2\sigma_\mathrm{p}+\sigma_\mathrm{n})/3(\mathrm{Z}\sigma_\mathrm{p}+\mathrm{N}\sigma_\mathrm{n})$ and was found [6] equal to 1.14±0.02 for ^{4}He and ^{12}C, and 1.18±0.02 for ^{56}Fe for the kinematic range of this measurement. The data is shown for Q^2 between 1.4 and 2.6 $(\mathrm{GeV/c})^2$, with

an average Q^2 value of ~1.6 (GeV/c)^2. For $x > 1.5$, there is high statistics data over a large range in Q^2, and it was observed [5, 6] that scaling was valid for $Q^2 > 1.4$ and $1.5 < x < 2$, as shown in Fig. 2.

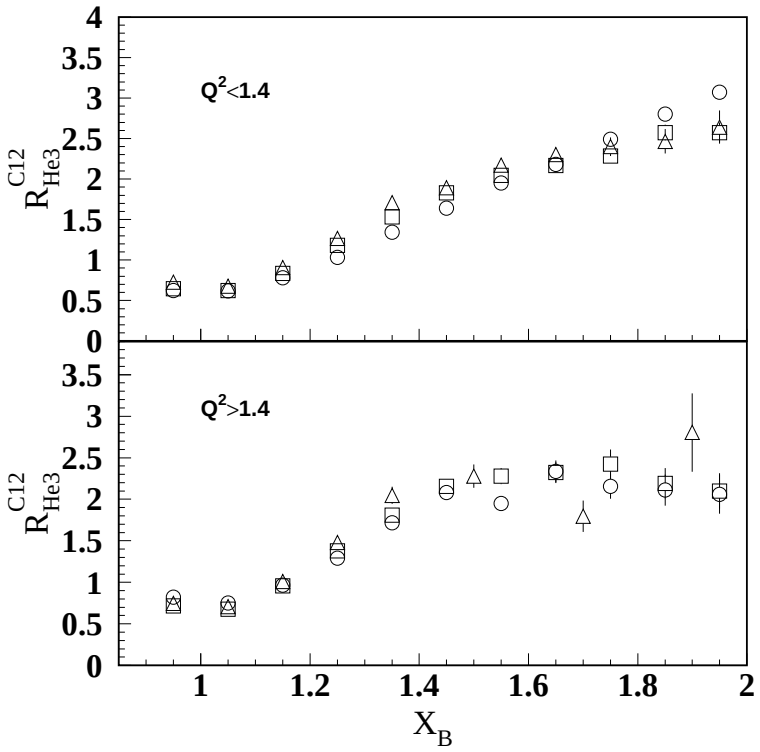

FIG. 2: Ratio of ^{12}C to ^3He cross sections for $Q^2 < 1.4$ GeV^2 (top) and $Q^2 > 1.4$ GeV^2 (bottom). Figure from Ref. [5].

For the 3N-SRC region, the cross section is much smaller, and data for $Q^2 > 1.4$ were combined, yielding a plateau in x, which suggests that the data are in the scaling region. The data from Ref. [6] (Fig. 1) provided the first direct indication of scaling in the x-region between 2.25 and 2.80, corresponding to dominance of three-nucleon short range correlations. But these data have limitations that make it difficult to make a quantitative extraction of the 3N-SRC probabilities, or even to ensure that the measurement is directly sensitive to the 3N-SRC contributions.

II. DETAILS OF PREVIOUS MEASUREMENTS

There have been several measurements in the 2N-SRC region, providing sufficient data to measure the relative 2N contributions in light and heavy nuclei, and to test the x and Q^2 dependence to verify scaling. While the only published results showing ratios of few-body and heavy nuclei to deuterium come from combining different measurements, Hall C experiments E89-008 and E02-019 made direct measurements of few-body and heavy nuclei to deuterium, and measured absolute cross sections in addition to ratios to help provide further tests of scaling and FSI contributions at large x. So while there are limitations with each of these previous extractions in the 2N-SRC region, the combined results from these measurements should give a relatively complete picture of most of the issues for 2N-SRCs. The main outstanding issue is the isospin dependence, discussed in Sec. III, where we can provide some new information in inclusive scattering to complement the two-nucleon knockout data from Hall A experiment E01-015 [7, 8].

The most recent CLAS data [6] provide the best measurement of 3N-SRCs, but there are limitations in the data. First, there was not enough data to look at the Q^2 dependence of the ratios, as most of the statistics are in the lowest Q^2 bin. Figure 3 shows the average values of a_2 (top) and a_3 (middle) extracted from the ratio of Fe/^{3}He for four Q^2 bins. For the 2N-SRC region we can see that the ratio is essentially Q^2 independent above 1.4 GeV^2, and also that the ratio is x-independent for each of these Q^2 bins (Fig. 2). For a_3, the average value is only precisely measured for

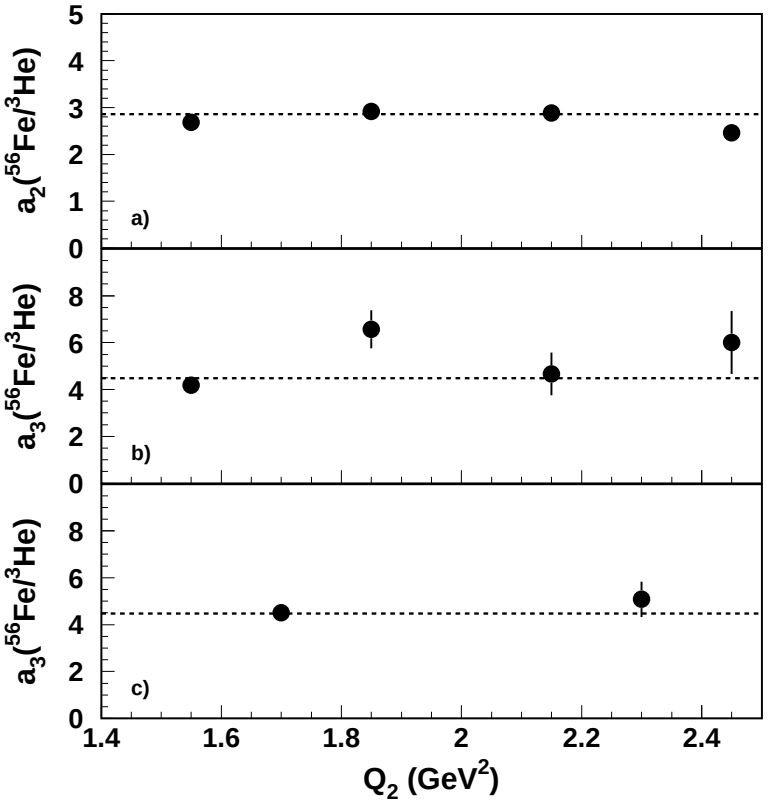

FIG. 3: Q^2-dependence of 2N (top) and 3N (middle) correlations for ^{56}Fe from recent JLab Hall B data [9]. The middle and bottom plots show the same data, but with different Q^2 binning. The plots show $a_j(^{56}\mathrm{Fe}/^3\mathrm{He})$, which is the ratio of $a_j(^{56}\mathrm{Fe})$ to $a_j(^3\mathrm{He})$ which are defined in Eqn. 1.

the lowest Q^2, and this value is ~30% below the average of the higher Q^2 bins, a disagreement of about 2.5σ. The statistics are such that there is no real verification of the Q^2-independence of the ratio, and in fact, some indication of a lack of scaling. Even if we assume that the results are independent of Q^2 above 1.4 GeV^2, the data (Fig. 1) do not allow us to set strong limits on the x dependence in this region, and so do not provide a verification of scaling in either the x or Q^2 dependence.

The experiment assumed that scaling set in for 3N-SRC at the same Q^2 as for 2N-SRC, and then averaged the data above $x = 2.25$. If one wants to isolate 3N-SRCs by probing above some minimum nucleon momentum, then for a reasonably large Q^2 value, there is an x value above which one probes above that minimum nucleon momentum [5], as one sees in Fig. 4. However, the x region at for which scaling is valid depends on the value of Q^2, and also on the target nucleus, especially for light nuclei. Given that we cannot study scaling as a function of Q^2 for this data, or even make a strong quantitative statement about the region of x above which scaling is observe, it is difficult to make a quantitative extraction of $a_3(A)$. As observed in Fig. 3, the lowest Q^2 point dominates the averaging. Thus, the result may not be reliable if the scaling region has not yet been reached. For example, the average of the three last points gives approximately $a_3(^{56}\mathrm{Fe}/^3\mathrm{He}) \approx 5.8 \pm 0.6$, compared to the lowest Q^2 point, which gives $a_3(^{56}\mathrm{Fe}/^3\mathrm{He}) \approx 4.2 \pm 0.2$. So 80–90% of the statistics come from the lowest Q^2 bin, which is approximately 2.5σ from the average of the higher Q^2 data. This is not strong enough to conclude that scaling is *not* valid, but makes it difficult to argue that scaling has been demonstrated at the level necessary for a quantitative extraction of the 3N-SRC probabilities. More precise data, especially at somewhat larger Q^2, are needed to precisely determine $a_3(\mathrm{A}/^3\mathrm{He})$ and to clarify its Q^2 and x dependence.

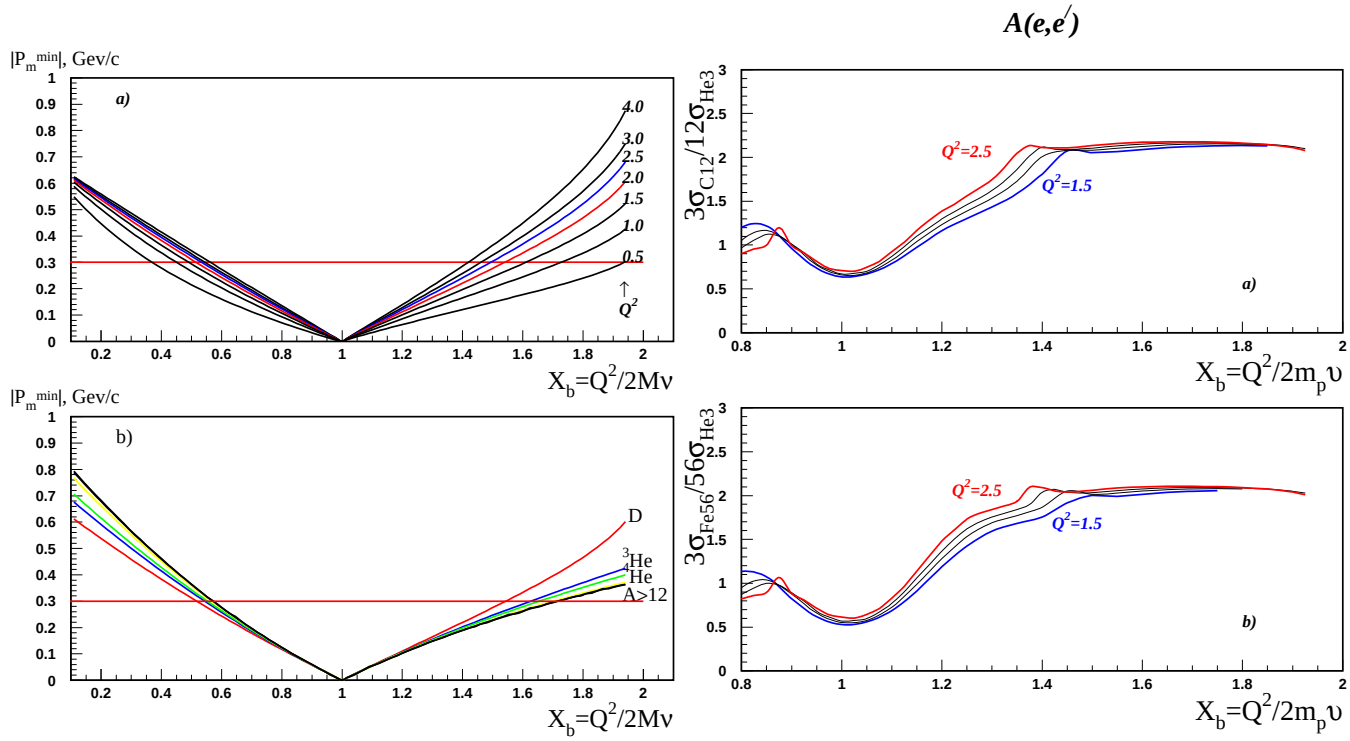

FIG. 4: Left: Minimum nucleon momentum probed as a function of x and Q^2 for deuterium (top) and as a function of x and A for $Q^2 = 2.0$ GeV^2 (bottom). Right: Plot showing calculated A/^{3}He ratio for four Q^2 values, showing the Q^2 dependence of the scaling region in x (from [10]).

Another issue that has not been examined in detail in these previous measurements is the choice of variables used in examining scaling. Most measurements have looked at these ratios only in terms of x. This is convenient as it *kinematically* separates regions involving two, three, or more nucleons. For deuterium, the cross section becomes zero for $x > 2$, and thus the contributions from an at-rest 2N-SRC is limited to $x \leq 2$. However, in a relativistic examination of scaling [4], it is more natural to study scaling in terms of α_{2N}, the light cone variable associated with the interacting nucleon belonging to the 2N-SRC:

$$\alpha_{2N} = 2 - \frac{q_- + 2m}{2m} \frac{\sqrt{W^2 - 4m^2} + W}{W}. \tag{3}$$

For $Q^2 \to \infty$, $\alpha_{2N} \to x$, but there is a significant difference for Q^2 values in the few GeV^2 range. One can see this in the plots on the right side of Fig. 4, where the onset of scaling at a constant value of α_{2N} yields an onset of scaling that shifts to lower x values at Q^2 increases. To examine the difference between scaling as a function of x and α_{2N}, one needs high statistics data with fine binning in x (α_{2N}) for several different Q^2 values. While the analysis of SLAC measurements [4] indicated improved scaling as a function of α_{2N}, there were relatively large uncertainties in that analysis, as it involved measurements from multiple data sets, extrapolated to common kinematics. The CLAS data [5, 6] examined scaling only as a function of x. With the proposed measurements, we will be able to study scaling in detail, test the prediction that α_{2N} is the better scaling variable and thus provides the best isolation of 2N-SRCs, and allow us to connect the region where 2N- or 3N-SRCs become dominant to the light cone momentum distributions. It also allows us to make optimal use of the data, as the use of the approximate scaling variable x requires that we limit ourselves to the scaling region of the *lowest* Q^2 data. For $x < 2$ and low Q^2, we can afford to exclude a significant portion of the x region to ensure that we are in the scaling region. This is not always possible when we extend these studies to higher Q^2 values or to the 3N-SRC region.

The expression for α can be generalized for multi-nucleon correlations [11]:

$$q_- \cdot \alpha_j m_N + q_+ \cdot (m_A - \frac{M_r^2}{m_N \cdot (j - \alpha_j)}) = m_N^2, \tag{4}$$

where α_j is the equivalent scaling variable for a j-nucleon SRC, and M_r is the mass of the recoil system of the residual (j-1) nucleons from the j-nucleon SRC. Taking $j = 3$ allows us to solve for α_{3N}, but the result depends on the value of M_r. The minimum value of the recoil mass, $M_r = 2 * m_N$, corresponds to a linear 3N-SRC configuration where the struck nucleon has the highest momentum, and its momentum is balanced by two nucleons going in the opposite direction. Higher values of M_r correspond to cases where the residual nucleons are not parallel, such as a symmetric star configuration. Thus, examining the scaling as a function of α_{3N} and varying the value of the recoil mass can provide sensitivity to the details of the 3N-SRC structure.

III. ISOSPIN EFFECTS ON SRC

Another recent topic of interest is the isospin dependence of short-range correlations. While the ratios shown in Figs. 1,2 are corrected for the difference between the electron-proton and electron-neutron cross sections, they assume that the ratio of neutrons to protons in the 2N-SRCs and 3N-SRCs is equal to the N/Z ratio of the nucleus. This is true if one assumes that the nature of the correlations is independent of the isospin. However, for 2N-SRCs, a global analysis [12] of the inclusive data discussed above and A(p,ppn) reactions [13, 14] as well as new results from ^{12}C(e,e'pN) measurements in Hall A [8, 15] suggest that 90% of the 2N-SRCs in ^{12}C are pn, while the nn and pp correlations provide only around 10% of the 2N-SRCs. Recent calculations [16] show that for 2N-SRCs at rest in a nucleus, the Tensor force yields an excess of high-momentum nucleons in deuteron-like (T=0) np correlations, while nn, pp, np pairs with T=1 are all strongly suppressed.

We can study these effects using inclusive scattering in the 2N-SRC (or 3N-SRC) dominated regions for nuclei with different N/Z ratios. Detailed calculations exist for few-body nuclei, and it is easy to see the impact of the isospin dependence for a simple case; the comparison of ^{3}He and ^{3}H. For isospin-independent 2N-SRCs, ^{3}He will have two pn pairs and one pp pair, compared to two pn pairs and one nn pair for ^{3}H. For ^{3}He, this yields four options for a high-momentum proton and two for a high-momentum neutron, yielding a proton distribution that is twice the neutron distribution at large momenta. For ^{3}H, the opposite happens, but in both cases, the ratio of the proton to neutron momentum distributions, $n_p(k)/n_n(k)$ at high momentum is just equal to the Z/N ratio for the proton. If deuteron-like SRCs dominate, then each nucleus has two pn pairs and negligible contributions from pp or nn pairs, yielding $n_p(k)/n_n(k) = 1$ for $k > k_F$. So for dominance of T=0 pairs, the cross sections in ^{3}He and ^{3}H at $x \gtrsim 1.5$ will be identical, while for the isospin-independent case, the ratio will be $(2\sigma_p + \sigma_n)/(\sigma_p + 2\sigma_n)$.

We can also see the impact of the isospin structure of the correlations in the calculated momentum distributions for the proton and neutron in ^{3}He. Figure 5 shows a calculation of the momentum distribution for protons and neutrons in ^{3}He, as well as their ratio [17, 18], using the Argonne v18 + Urbana IX two-nucleon and three-nucleon potentials. For the isospin-independent case, the proton-to-neutron ratio would always be Z/N = 2. In the case of dominance of the T=0 np pairs, the ratio for $k \gg k_F$ would equal 1. The calculation predicts that the ratio at high momenta, where 2N-SRCs dominate, is approximately 1.5 at the largest momentum, with a weighted average closer to 1.2 for $k > k_F$. This suggests a significant excess of np pairs over what one would expect from isospin-independent interactions, but not a total dominance of the T=0 pairs. This can be studies in the region where 2N-SRCs dominate, as well as the region of 3N-SRC dominance, where more possible isospin configurations are possible for the 3N clusters.

The ideal case for studying the isospin dependence is the comparison of ^{3}H to ^{3}He, as there is a large difference in the N/Z ratio, with otherwise essentially identical density and structure. Such measurements should be possible using the moderate-density ^{3}H target proposed for E12-06-118 [19]. Because of the lower density of the target, it will be important to know what Q^2 is required to reliably access the scaling region for both 2N and 3N-SRCs, making the measurements proposed here valuable for designing such an experiment, as well as optimizing the approved measurement E12-06-105 which will make measurements at $x > 2.5$ for a variety of few-body and heavy nuclei. In the

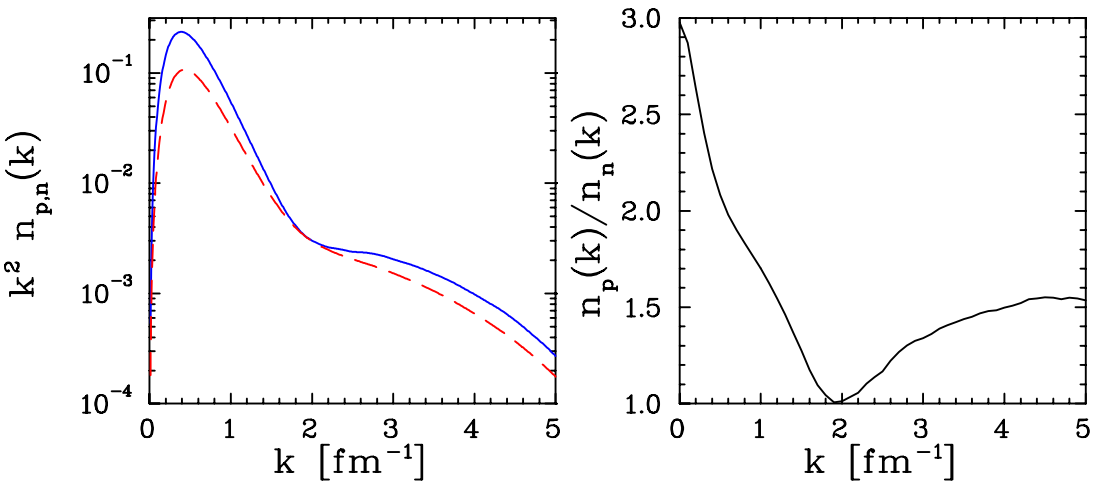

FIG. 5: Left: Momentum distribution for protons (solid) and neutrons (dashed) in ^{3}He from Quantum Monte Carlo calculation [17, 18]. Right: Ratio of proton to neutron distributions.

meantime, we can make similar measurements using heavier nuclei (^{40}Ca and ^{48}Ca), which also cover a large range in the ratio of N/Z for nuclei that are very similar in mass. Because the radii of ^{40}Ca and ^{48}Ca are similar, the proton density is similar for the two isotopes, while the neutron density is higher.

For the kinematics of this measurement, the cross section for scattering from a proton is approximately three times the cross section for scattering from a neutron. If the ratio of protons to neutrons at large momenta goes like N/Z, then the cross section per nucleon should be approximately 8% lower for ^{48}Ca, due to the 40% increase in the number of neutrons:

$$\frac{\sigma(\mathrm{e}-^{48}\mathrm{Ca})/48}{\sigma(\mathrm{e}-^{40}\mathrm{Ca})/40} = \frac{(20\sigma_p + 28\sigma_n)/48}{(20\sigma_p + 20\sigma_n)/40} \approx \frac{(20\sigma_p + 28\sigma_p/3)/48}{(20\sigma_p + 20\sigma_p/3)/40} = 0.916. \quad (5)$$

If we take the case where only np correlations matter for large x, then there are 20*20 possible np pairs in ^{40}Ca and 20*28 in ^{48}Ca. Scaling to the number of nucleons, this gives

$$\frac{\sigma(\mathrm{e}-^{48}\mathrm{Ca})/48}{\sigma(\mathrm{e}-^{40}\mathrm{Ca})/40} = \frac{(20*28)/48}{(20*20)/40} = 1.17, \quad (6)$$

or a 17% increase in the cross section per nucleon for ^{48}Ca, compared to the isospin-independent expectation of an 8.4% decrease. This assumes that any pair of nucleons can be part of a correlated pair, while the fact that the ratio of A/^{2}H saturates at a value of 5–6 implies that only a certain number of "nearest neighbors" are involved in forming SRCs. However, the ratio of neutrons to protons for the "nearest neighbors" will scale with the total number of neutrons and protons, yielding identical results if we limit ourselves to a subset of participant nucleons in determining these ratios. There will also be a small correction due to the difference in the ratio of surface to volume between ^{40}Ca and ^{48}Ca. Because the number of 2N-SRCs depends only weakly with A for heavier nuclei, Ref. [4] extracts $a_2(^{12}\mathrm{C})$=5.0±0.5, $a_2(^{197}\mathrm{Au})$=4.8±0.7, the correction due to the mass difference between ^{40}Ca and ^{48}Ca will be negligible compared to the 25% difference between the expectation for isospin-independent and isospin-dependent (T=0 dominance) models. While the comparison to theory is more difficult, the sensitivity is not too much worse than the comparison of ^{3}H to ^{3}He, where there is a 40% difference between $T = 0$ dominance (^{3}H/^{3}He=1) and the isospin-independent case ($^3\mathrm{H}/^3\mathrm{He} = (2\sigma_p + \sigma_n)/(\sigma_p + 2\sigma_n) \approx 1.4$ for $\sigma_n/\sigma_p \approx 0.3$).

Recently theoretical efforts have been put into the expression of the equation of state for asymmetric nuclear matter which is essential in the understanding of neutron stars. One of the challenging features of this theoretical work is to address the nucleon-nucleon interaction behavior in symmetric nuclear matter and in pure neutron matter. In the approach of Ref. [20], they predict a significant difference between the neutron and proton momentum distributions

for an asymmetric factor (N-Z)/A of 0.2, corresponding to ^{48}Ca. This calculation is in good agreement with previous experimental results showing that protons are more affected by correlations due to interactions with out-numbered neutrons.

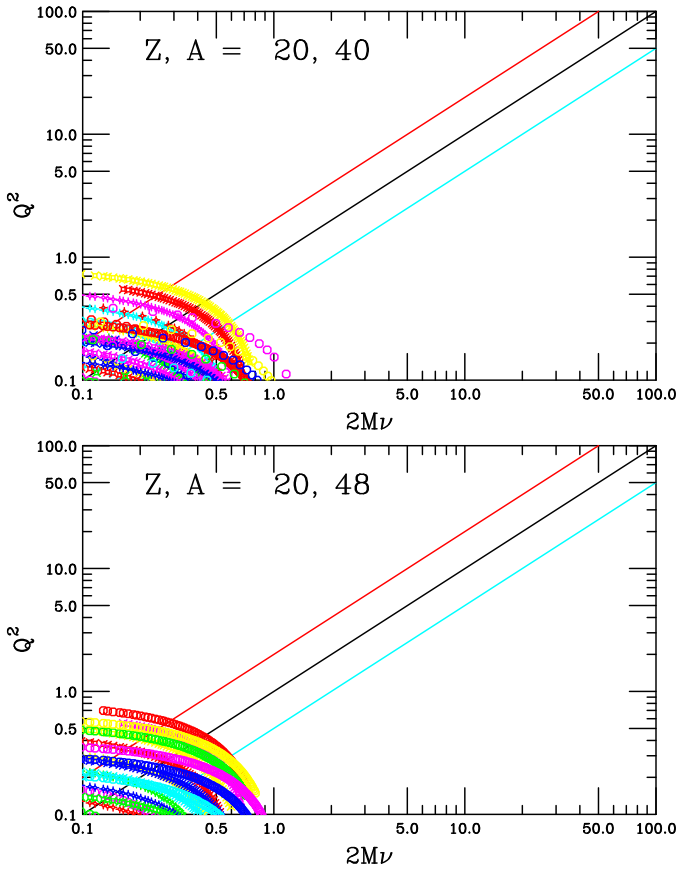

FIG. 6: Kinematic coverage of existing ^{40}Ca and ^{48}Ca data as a function of Q^2 and $2M\nu$. The middle (black) line shows x=1, while the top (red) line shows x=2.

Figure 6 shows the kinematic coverage of existing data on ^{40,48}Ca. While the proposed measurements on ^{3}He and the A/^{3}He will provide significant improvements over previous measurements, the existing data on ^{40,48}Ca is entirely limited to lower Q^2, and no such measurements of the isotopic dependence of the correlations exist for medium or heavy nuclei. The only data looking at the isotopic dependence of SRCs is the comparison of ^{3}He and ^{4}He in the CLAS data and the E02-019 results which are limited in their precision and kinematic coverage. In addition, ^{3}He and ^{4}He differ significantly in size and average density, and so we expect very different values of $a_{2,3}(^3\text{He})$ and $a_{2,3}(^4\text{He})$ even for isospin-independent SRCs. Finally, the A dependence of the minimum momentum probed for a given x and Q^2 setting is strong for light nuclei, but weak for heavier nuclei (left plot, bottom panel of Fig. 4), making it critical for the comparison of few-body nuclei that the (A-dependent) scaling region has been reached for the lightest nuclei.

IV. THE PROPOSED MEASUREMENT

We propose to perform precision measurements of the inclusive electron scattering cross sections for ^{2}H, ^{3}He, ^{4}He, ^{12}C, ^{40}Ca and ^{48}Ca with an incident beam energy of 3.6 GeV and at eight scattering angles: 15°, 17°, 19°, 21°, 23°, 25°, 27° and 29°. Our focus is on the $x > 2$ region; Fig 7 shows the x and Q^2 coverage of the proposed experiment.

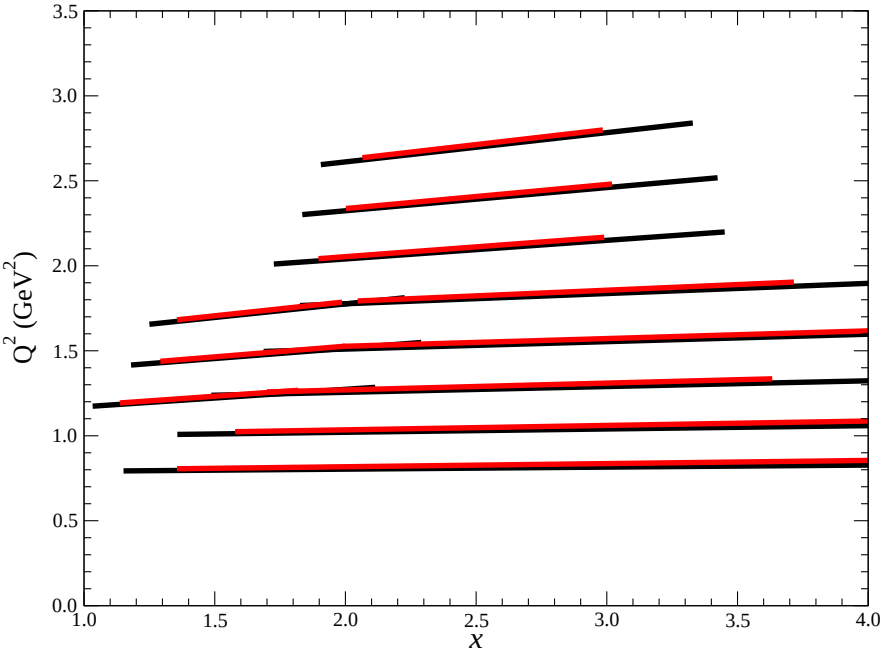

FIG. 7: Proposed kinematic coverage. In red is shown the central ±3% of the HRS momentum acceptance, and in black the full acceptance region of ±4.5%

A. Background

Cryo-target: aluminum window contribution

The ^{2}H, ^{3}He and ^{4}He cryo-targets are contained in 20cm aluminum cans made from aluminum 7075-T6 of density of about 2.8 g/cm^3. The aluminum windows are equivalent to ≈13% of the ^{3}He thicknesses (Table I). Because the ratio of the Al to ^{3}He cross sections in the 3N-SRC region is roughly 3–4 (based on Fig. 1), the Al contribution is approximately 45% of the ^{3}He cross section on the ^{3}He target, so contributes ≈35% of the total cross section. Fig. 8 illustrates the contamination of the aluminum window in a 4cm ^{3}He cell. In the region of interest of our proposed measurement ($x \gtrsim 2.3$), the endcap contributes more than half of the total cross section. By using a 20cm cell, we should be able to reduce this contribution by at least a factor 5. Moreover, the resolution of the two HRS allows us to perform a software cut to remove the endcap contributions. We also plan to take data on an empty aluminum can with the same thicknesses to test the efficiency of the cuts, and to subtract any residual endcap contribution. We can also test this by removing the software cuts and subtracting the full endcap contribution.

Target	T(K), P(psia), L(cm)	Thickness(g/cm^2)
^{2}H	22.0, 22.0, 20.0	3.35
^{3}He	8.0, 200.0, 20.0	1.38
^{4}He	8.0, 200.0, 20.0	2.28
Al Entrance	N/A, N/A, 0.035	0.09
Al Exit	N/A, N/A, 0.035	0.09
Al Wall	N/A, N/A, 0.035	0.09

TABLE I: Aluminum window/wall thickness and running conditions of the cryo-target (from [21])

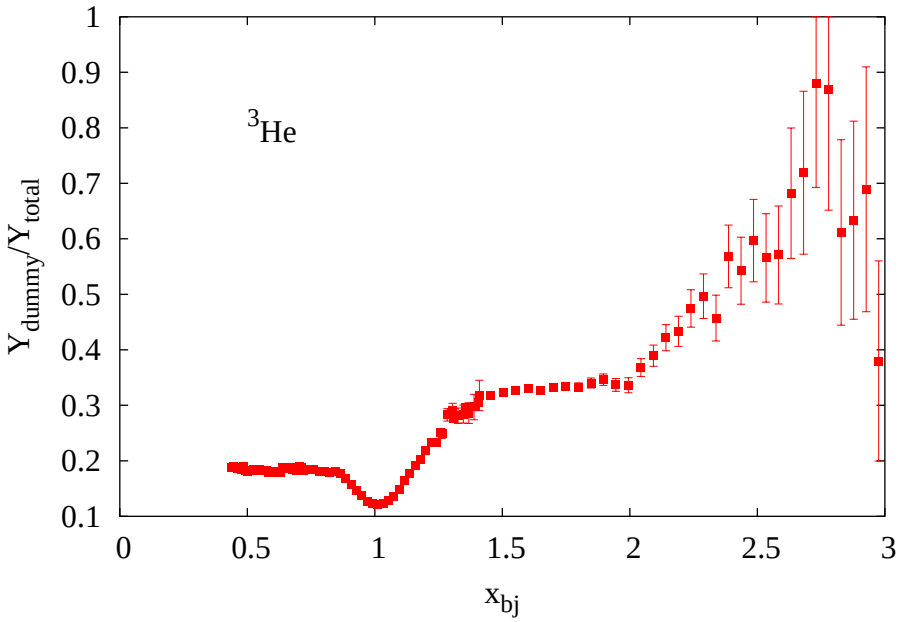

FIG. 8: Dummy contamination from JLab Experiment E02-019 data for a 4cm cell. Plot from Ref. [22].

Pion contamination and charge-symmetric background

The expected pion background has been evaluated using experimental data of JLab Experiment E89-008 [23]. For an incident energy of 4.045 GeV and at a scattering angle of 23°, the π/e ratio was found to be approximately 10:1 for a 2% RL carbon target at a momentum setting of 3.76 GeV and 4:1 for a 2% RL iron target at 3.60 GeV.

The PID performance of Hall A HRS detectors has been shown to be very good in past experiments (see [24, 25], for example) allowing a reduction of the pion background by a factor of about 10^4, while keeping an electron efficiency better than 99%, when CO_2 gas Čerenkov counter and double-layer lead glass calorimeter are associated. This yields a worst-case pion contamination of ≈0.1%.

The charge-symmetric background can be very large for large scattering angles, but decreases rapidly at smaller angles. For E02-019 [22], the charge-symmetric background for even the high-Z, 6% radiation length targets was always well below 1% for angles below 30° and relatively large values of x ($x \gtrsim 0.6$). For the targets proposed here and scattering angles below 25°, we expect a maximum charge-symmetric background to be below 0.1%.

B. Projected results

To estimate the coverage and the precision of the proposed measurements, a conservative momentum bite of ±3% was used. This is sufficient to fully cover the 3N-SRC region in one setting, although using the full HRS momentum acceptance will improve the coverage in the 2N-SRC region and also expand to the x>3 region. The data were binned in x with a binsize of 0.1. Respecting the beam current allowed on each target (see Table II) and data acquisition limit (3.5kHz assuming the same DAQ configuration as during E97-110), the projected statistical uncertainties were estimated after optimizing the limited time available for the measurements. For the cryo-target, the beam current limitation is due to the coolant restriction.

The rates for ^{3}He were evaluated using the XEM cross section model [22] based on y-scaling for the large x region. The XEM model was fitted to data on a variety of light and heavy nuclear targets for both the DIS and $x > 1$ region, but with a beam energy of 5.8 GeV. Figure 9 shows a comparison of the model with existing data for ^{3}He [26] at lower Q^2, closer to the range of the proposed measurements. At these lower Q^2 values, the model is still in good

Target	T (K)	P (psia)	length (cm)	RL (g/cm^2)	I^{limit} (μA)
^{2}H	22.0	22.0	20.0	3.35	60.0
^{3}He	8.0	200.0	20.0	1.38	60.0
^{4}He	8.0	200.0	20.0	2.28	60.0
	thickness (cm)				
^{12}C	0.50			0.95	80.0
^{40}Ca	0.43			0.66	40.0
^{48}Ca	0.43			0.66	40.0

TABLE II: Cryo-target characteristics from [21] (top part) and, solid targets and their characteristics asked for this proposal (bottom part).

agreement with the data from SLAC [27]. While the model is fit to the E02-019 kinematics (3–4 GeV^2), it is good at approximately the 20% level down to Q^2 values below 0.5 GeV^2 based on a comparison to the database [26] and also at higher Q^2 values between 1.0 and 4.0 GeV^2 [24].

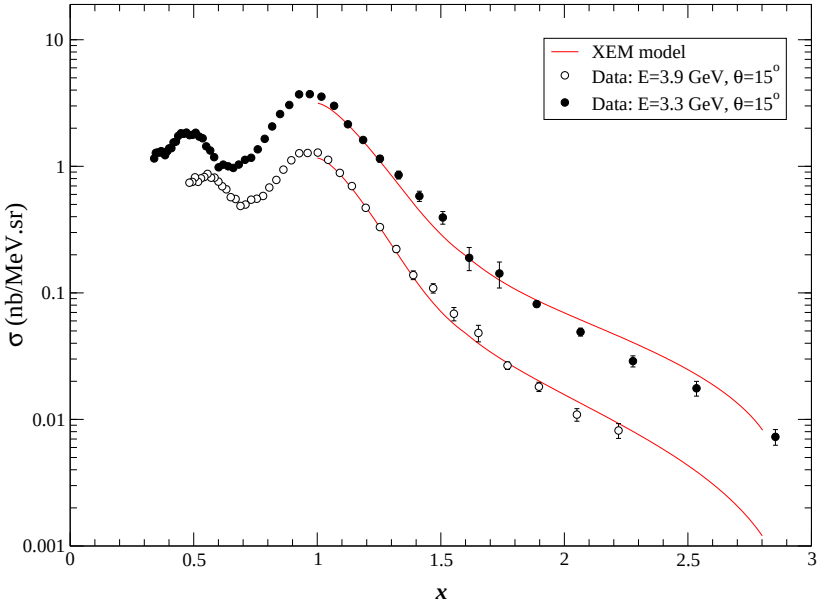

FIG. 9: Comparison of the XEM cross section model with ^{3}He world data from [26].

The cross sections for heavier nuclei (^{4}He, carbon and calcium isotopes) were estimated using the XEM model for ^{3}He and the ratio A/^{3}He from the Hall B SRC results. Considering that the scaling factor between the model and Hall B at a given x for the nucleus $A > 3$ is S_A, we can write:

$$S_A \cdot r^{model}_{A/3He} = r^{HallB}_{A/3He} \quad \Rightarrow \quad S_A \cdot \sigma^{model}_{A>3} = \sigma^{HallB}_{A>3}. \tag{7}$$

The resulting uncertainty on the ratio from the scaled model will be expressed as follows:

$$\Delta r_{A/3He} = r^{HallB}_{A/3He} * \sqrt{\left(\frac{\Delta\sigma^{model}_A}{\sqrt{S_A}\cdot\sigma^{model}_A}\right)^2 + \left(\frac{\Delta\sigma^{model}_{3He}}{\sigma^{model}_{3He}}\right)^2}. \tag{8}$$

For calcium isotopes, a logarithmic extrapolation with respect to A was done to estimate the values of $a_2(^{40,48}\text{Ca}/^3\text{He})$ and $a_3(^{40,48}\text{Ca}/^3\text{He})$. Then the ^{40,48}Ca cross sections from the model were scaled using the same procedure as above. These estimates do not account for any isotopic dependence in the cross section, and so yield

essentially identical values for ^{40}Ca and ^{48}Ca, rather than the 25% difference one would expect if np correlations dominate and one follows the same approach as in the past, i.e. applying the naive correction for the neutron excess based on the N/Z ratio.

The ^{2}H, ^{4}He, carbon and calcium isotopes target running times were optimized by requiring that the contribution of the relative uncertainty from nucleus A is equal to the ^{3}He one in Eq (8), or:

$$\frac{\Delta\sigma_A}{\sqrt{S_A}\cdot\sigma_A} = \frac{\Delta\sigma_{3He}}{\sigma_{3He}}. \tag{9}$$

For ^{2}H, a similar procedure was used to determine the running time by using ^{3}He/D ratio results from ref. [4] as a scaling factor for the deuterium cross sections.

The angular acceptance $\Delta\Omega$ was estimated at 3.2msr and a conservative momentum bite ΔP of $\pm$3% and an effective cryo-target length of 15cm were chosen to evaluate the physics rates. The estimate time needed at each of the eleven kinematic settings is given in Tables III- IV, as well as the beam currents (I), the total rates (R_{tot}) after prescaling by the factor psc (also listed) and the physics rates (R_{phys}). Note that, only for the kinematic setting at 29°, the total running time needed is splitted between the left and the right HRS.

θ (deg)	E' (GeV)	x_{range}	Q^2_{range} (GeV/c)^2	Tg	I (μA)	psc	R_{tot} (Hz)	R_{phys} (Hz)	time (hrs)	Total (hrs)
21.0	3.100	1.3-2.0	1.44-1.53	3	60	1	1517	333	3.0	
				2	60	1	2571	522	2.4	
				4	60	1	3085	811	1.1	
				12	80	1	1858	726	1.2	
				40	40	1	716	283	2.9	
				48	40	1	678	268	3.1	**13.7**
23.0	3.030	1.4-2.0	1.68-1.79	3	60	1	383	88	6.0	
				2	60	1	568	125	4.8	
				4	60	1	829	226	2.1	
				12	80	1	509	206	2.3	
				40	40	1	198	81	5.8	
				48	40	1	188	77	6.2	**27.2**
27.0	3.070	2.0-3.0	2.34-2.48	3	60	1	2.4	0.5	42.0	
				4	60	1	6.0	1.4	12.4	
				12	80	1	4.0	1.3	12.8	
				40	40	1	1.6	0.6	27.6	
				48	40	1	1.5	0.5	28.6	**123.4**
29.0	3.010	2.1-3.0	2.64-2.80	3	60	1	0.7	0.1	21.0	
				4	60	1	1.7	0.4	6.2	
				12	80	1	1.1	0.4	6.4	
				40	40	1	0.5	0.2	13.8	
				48	40	1	0.4	0.2	14.3	**61.7**
								Total time needed (RIGHT)		**226.0**

TABLE III: List of kinematics for right HRS and estimated beam time needed for the proposed experiment. The right arm running is simultaneous to the left arm running, and so does not increase the total time needed.

θ (deg)	E' (GeV)	x_{range}	Q^2_{range} (GeV/c)^2	Tg	I (μA)	psc	R_{tot} (Hz)	R_{phys} (Hz)	time (hrs)	Total (hrs)
15.0	3.385	1.4-4.0	0.81-0.86	3	60	8	3377	485	2.0	
				2	60	14	3324	369	2.8	
				4	60	16	3420	639	1.2	
				12	80	10	3352	934	0.8	
				40	40	4	3194	926	0.7	
				48	40	4	3023	880	0.7	**8.2**
17.0	3.355	1.6-4.0	1.02-1.09	3	60	1	2582	421	2.4	
				2	60	1	3100	412	1.9	
				4	60	2	3045	603	1.4	
				12	80	2	1984	561	1.5	
				40	40	1	1538	455	1.6	
				48	40	1	1462	433	1.6	**10.4**
19.0	3.135	1.1-1.8	1.19-1.27	3	60	4	2769	710	2.4	
				2	60	8	3415	793	3.8	
				4	60	6	3217	957	1.3	
				12	80	4	2753	1217	0.9	
				40	40	2	2051	921	1.2	
				48	40	2	1930	869	1.2	**10.8**
19.0	3.305	1.7-3.6	1.26-1.34	3	60	1	488	90	3.0	
				2	60	1	522	79	2.4	
				4	60	1	1196	260	0.9	
				12	80	1	793	242	0.9	
				40	40	1	309	99	2.0	
				48	40	1	294	94	2.0	**11.2**
21.0	3.275	1.9-3.8	1.52-1.61	3	60	1	76	13	6.0	
				4	60	1	188	39	1.8	
				12	80	1	128	37	1.8	
				40	40	1	50	16	3.9	
				48	40	1	47	15	4.1	**17.6**
23.0	3.230	2.0-3.7	1.79-1.90	3	60	1	15	2.5	12.0	
				4	60	1	39	7.8	3.5	
				12	80	1	27	7.4	3.7	
				40	40	1	10	3.2	7.9	
				48	40	1	10	3.1	8.2	**35.3**
25.0	3.120	1.9-3.0	2.04-2.17	3	60	1	10	2.0	24.0	
				4	60	1	25	5.9	7.1	
				12	80	1	17	5.6	7.3	
				40	40	1	6.6	2.3	15.7	
				48	40	1	6.3	2.2	16.4	**70.5**
29.0	3.010	2.1-3.0	2.64-2.80	3	60	1	0.7	0.1	21.0	
				4	60	1	1.7	0.4	6.2	
				12	80	1	1.1	0.4	6.4	
				40	40	1	0.5	0.2	13.8	
				48	40	1	0.4	0.2	14.3	**61.7**
							Total time needed (LEFT)			**225.7**

TABLE IV: List of kinematics for left HRS and estimated beam time needed for the proposed experiment.

Systematic	$\delta\sigma/\sigma$	$\delta R/R$ (normalization)	$\delta R/R$ (pt-to-pt)
Acceptance correction	2.0%*	0.5–2.0%	0.0–1.0%
Radiative correction	3.0%*	-	0.3%
Tracking efficiency	1.0%*	-	0.2%
Trigger efficiency	0.5%*	-	0.1%
PID efficiency	1.5%*	-	0.2%
Target thickness	0.5-2.0%	1.1–2.0%	-
Charge measurement	0.5%	-	0.5%
Energy measurement	0.05%	-	-
COMBINED UNCERTAINTY	4.1-4.6%	1.2-2.8%	0.7–1.2%

TABLE V: Relative systematic uncertainties in the extraction of the unpolarized cross sections from E01-012 [24] and of the cross section ratio from E03-103 [28]. Entries with an asterisk indicate corrections made directly on the cross section. Entries without asterisk indicate contributions to the overall uncertainty. For the target ratios, the acceptance correction is dominated by the target length acceptance, so is 2% for different length targets, and 0.5% when taking the ratio of two long targets (^{3}He/^{2}H) or two solid targets.

Table V summarizes the systematic uncertainties for this measurement. The normalization uncertainties come mainly from the uncertainty in target thicknesses, and the difference in the acceptance for short and long targets. The uncertainty in the charge measurement will yield an overall normalization in the ratio for a given Q^2 setting, and so will not modify the x dependence. However, it can vary over time and thus be different at different Q^2 settings, and so we are conservative and treat this, as well as most other systematic uncertainties, as point-to-point uncertainties. When we are specifically examining just the x dependence, the point-to-point uncertainties will be reduced.

The projected statistical uncertainties from the run times listed in Tables III-IV are plotted in Fig. 10. In Fig. 12, we show the uncertainties and Q^2-coverage we can achieve in the study of the Q^2-dependence of $a_3(\mathrm{A}/^3\mathrm{He})$. We also show $a_2(\mathrm{A}/^3\mathrm{He})$, even though it is not the primary goal of the proposed experiment, and we are planning to obtain the same precision for $a_2(\mathrm{A}/^2\mathrm{H})$ as shown in Fig. 11. We also plotted in Fig. 10 the projected statistical uncertainties for the ratios ^{40}Ca/^{12}C, ^{48}Ca/^{12}C and ^{48}Ca/^{40}Ca which will be of great interest in the understanding of the isospin dependence of the short-range correlations. In addition, we can form the ratios ^{12}Ca/^{4}He and ^{40,48}Ca/^{4}He as projected in Fig. 13. In the ratios A/^{4}He, it is expected that the 3N-motion effects partially cancel and therefore these ratios would exhibit a clearer scaling above x$\approx$2.25. In addition, it allows for ratios of heavy and light isoscalar nuclei, making these ratios free of any ambiguity associated with the issue of isospin dependence.

The CLAS measurements had statistical uncertainties of $\approx$5% and experimental systematic uncertainties of $\approx$7%. This does not include corrections for Coulomb distortion, estimated to be $\approx$5% for the data on iron. It also assumed that $Q^2 > 1.4$ GeV^2 and $x > 2.25$ were sufficient to be in the scaling region, although the result for iron would change by more than 30% and the statistical uncertainties grow significantly if a cut of $Q^2 > 1.7$ GeV^2 were applied (Fig. 3).

If we ignore the issue of validity of the scaling assumption, the uncertainty on the experimental ratio of cross sections is $\approx$10%. There are greater systematic uncertainties in their extraction of the SRC probability from the experimental yield ratios. The combination of Coulomb corrections and SRC-motion, which were estimated but *not* applied, along with the experimental systematics due to combining data from different run periods, led to a total uncertainty of $\approx$25%. We will achieve much better statistics, allowing for a careful examination of the x and Q^2 dependence. Because we will take most of the data at one time (only ^{2}H and ^{4}He are taken separately), with no kinematic changes between targets, the experimental systematics on the measured cross section ratios will be at the 2–3% level or better. In extracting the relative strength of the 3N-SRC configurations, we will apply corrections for Coulomb distortion and center-of-mass motion of the SRC, which will yield *total* uncertainties on the ratio of 3N-SRC of $\sim$10%, dominated by the uncertainty in these corrections. Thus, both the direct experimental ratios and the extracted information on the relative contributions of 3N-SRCs will be a factor of two or more better than the published CLAS results.

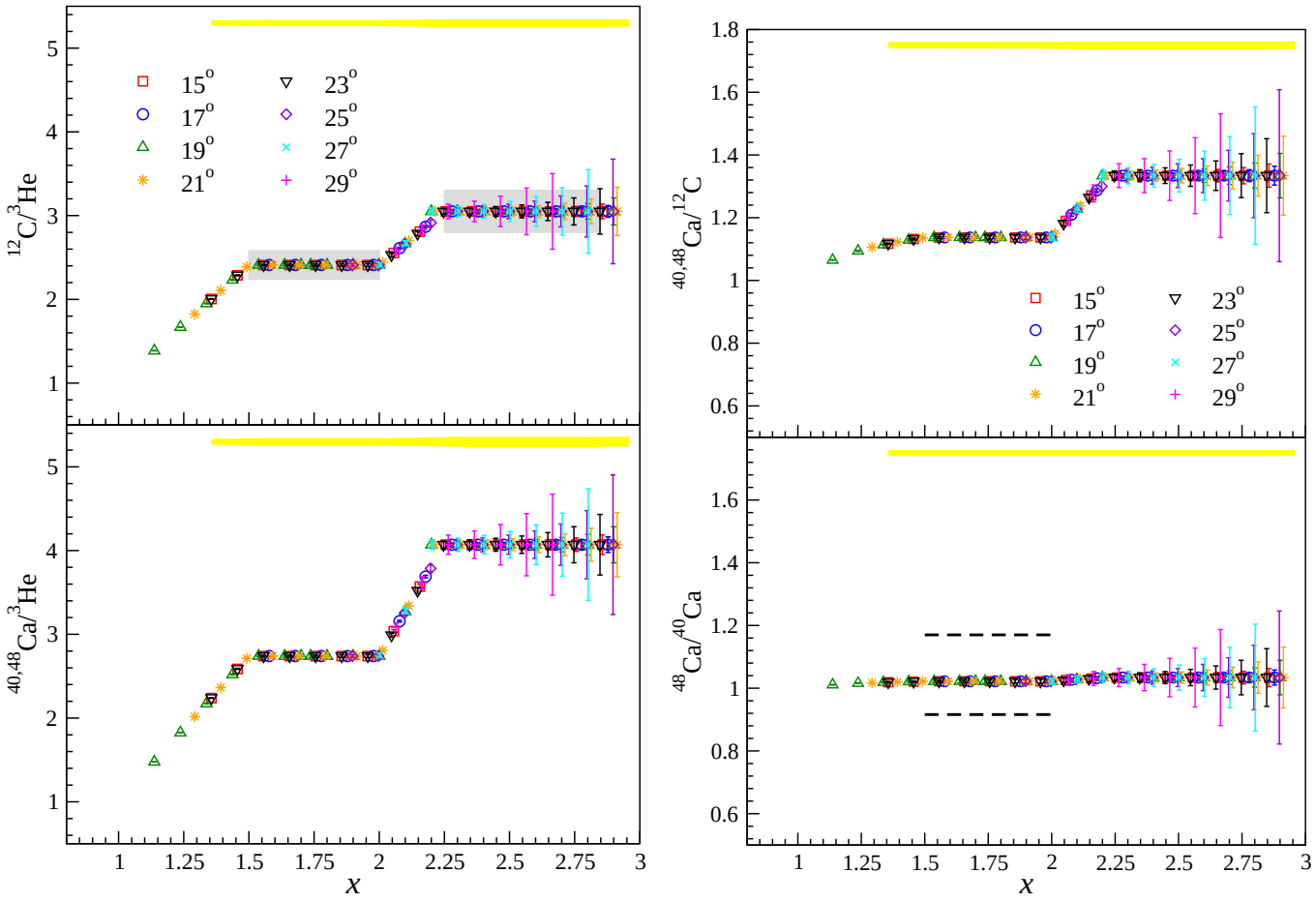

FIG. 10: Projected statistical uncertainties for data taken at a beam energy of 3.6 GeV and at the 8 scattering angles. The grey bands represent the resulting fits of the 2N and 3N correlations from recent JLab Hall B data [6]. The yellow bands represent a point-to-point systematic uncertainty of ±1.2% (±0.7% for ratios of solid targets). The error band does not include the overall normalization uncertainty of 1.3–2.9%, dominated by the uncertainty in the relative target thicknesses. The dashed lines for the ratio of ^{48}Ca to ^{40}Ca are the predictions assuming that the cross section simply differs by the difference in proton and neutron cross sections (bottom line), or the case where the cross section in the 2N-SRC region is dominated by pn pairs.

The CLAS measurement extracted only the normalized yield ratios, it did not measure the cross sections for the individual targets. Measurements of the absolute cross section for ^{2}H as $x \to 2$ and ^{3}He as $x \to 3$ will provide additional information that can be used to study the impact of final state interactions on the inclusive cross section in the 2N and 3N-SRC regions. While FSI are expected to be limited to interactions between the nucleons in the SRC, and thus cancel in the target ratios, this assumes that there is no isospin dependence in the FSI. Thus, comparisons to cross section calculations using realistic ^{3}He distributions will allow us to determine the size of FSI, or else to set limits on the size of FSI. For ^{2}H, a significant amount of data exist for moderate Q^2 and $x \to 2$, which allow us to map out the Q^2 dependence of these FSI, and which show that for larger Q^2, there is no indication of significant FSI contributions, even between nucleons in the 2N-SRC. The proposed measurements will allow for improved studies of the analogous case for 3N-SRC in ^{3}He, where we have a reliable baseline for the cross section in the absence of FSI.

Finally, these measurements will provide the first extraction of the ratios for $x > 3$, in the region where 4N-SRCs are expected to dominate. Using the full momentum acceptance, we have good coverage above $x = 3$ for the lowest Q^2 values, and some higher Q^2 settings can be easily be extended to slightly larger x than shown in Fig. 7. The settings were chosen to have good overlap between the left arm and right arm settings using just the central ±3% acceptance. Using more of the ±4.5% acceptance allows us to reduce this overlap for the intermediate Q^2 values where the cross

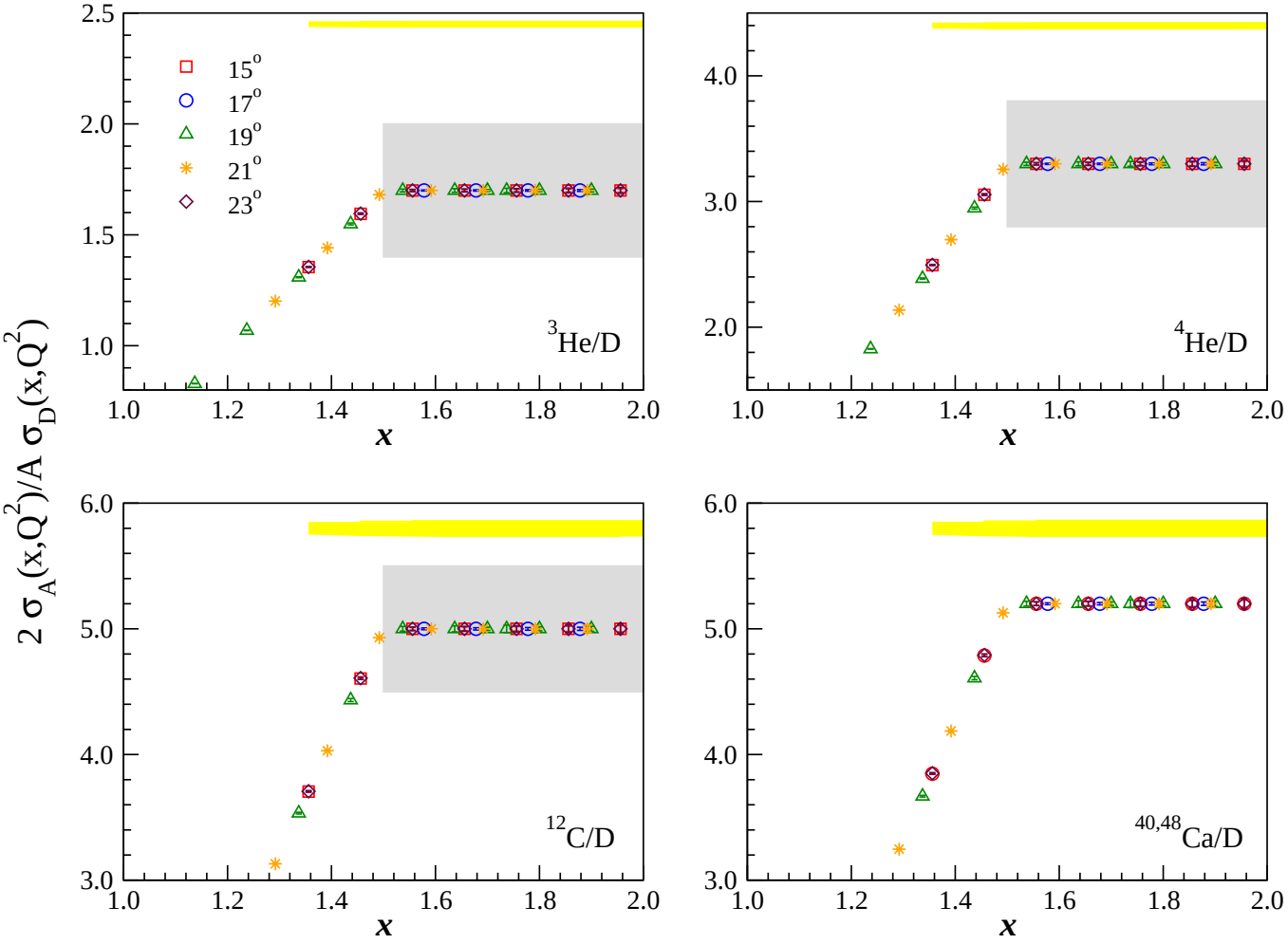

FIG. 11: A/D ratios projected statistical uncertainties for data taken at a beam energy of 3.6 GeV and at the 5 scattering angles. The grey bands represent the resulting fits of the 2N correlations from SLAC data [4]. The yellow bands represent a point-to-point systematic uncertainty of ±1.2% (±0.7% for cryo-target ratios), both slightly worse than we project for the final systematics. There is also an overall normalization uncertainty of 1.3–2.9% that is not shown.

section is sufficient to make useful measurements at higher x values. It is hard to predict what we will see, as we do not have reliable cross section estimates for this region, and we will be limited to somewhat lower Q^2 values. However, the initial exploration of the ratios in these kinematics will provide a first look at scaling, or at least the approach to scaling, in this region. This will be certainly be useful in providing guidance for the 12 GeV measurements that will reach significantly higher Q^2. In addition, given the tight binding of α-like clusters, the contribution of 4N-SRCs may be be stronger than one might naively expect, and thus there is the possibility of interesting results from even these initial explorations.

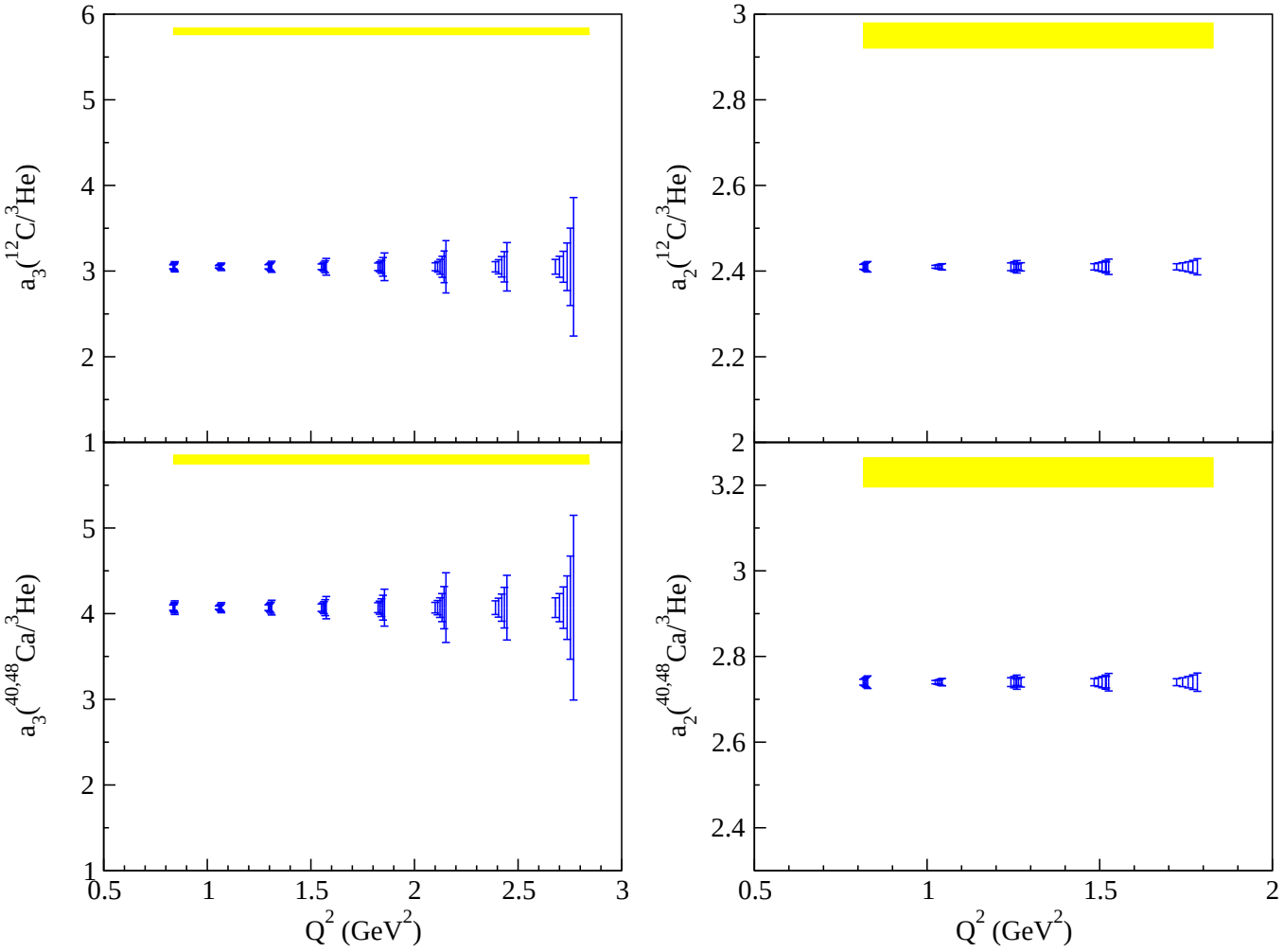

FIG. 12: Projected statistical uncertainties on the Q^2-dependence of the 3N SRC (left plots) for all 8 scattering angles. The y-axis scale was chosen to match Fig. 3, which had average Q^2 of 1.4–1.5 $(\mathrm{GeV/c})^2$. The 2N SRC projected statistical uncertainties are shown on the right plots. The yellow bands represent the point-to-point systematic uncertainty of ±1.2%. The overall normalization for each ratio of approximately 2–3% is not included, but does not impact the measurement of the x dependence of Q^2 dependence of the ratios. Note that for the isospin dependence studies, a direct comparison of ^{40}Ca and ^{48}Ca can be made, yielding point-to-point uncertainties of ±0.7% and a smaller normalization uncertainty due to the better cancellation in the acceptance correction for the two short targets.

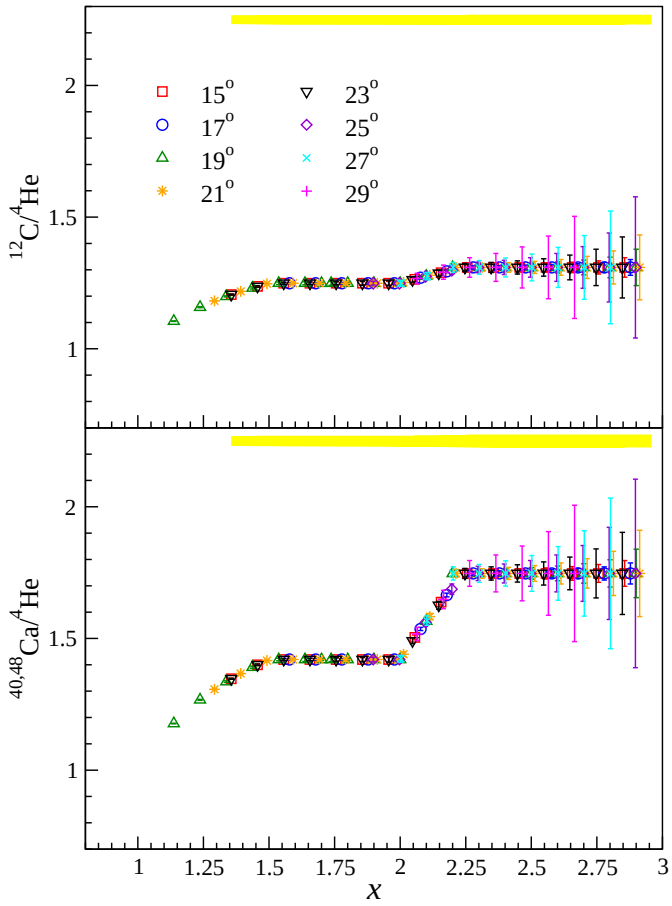

FIG. 13: A/^{4}He ratios projected statistical uncertainties for data taken at a beam energy of 3.6 GeV and at the 8 scattering angles. The yellow bands represent a point-to-point systematic uncertainty of ±1.2%. The error band does not include the overall normalization uncertainty of 1.3–2.9%, dominated by the uncertainty in the relative target thicknesses. Only expected results for $x < 3$ are shown here.

C. Overhead time

The total overhead time needed for calibration, background study and configuration changes is now evaluated.

Calibration and background studies

We will need to measure the contributions from the aluminum entrance and exit windows of the cryo-target. For each kinematic, 20% of the ^{3}He running time should be enough to accomplish a precise dummy subtraction. Taking into account the parallel running of the left and right HRS, the time needed for dummy running is 15 hours.

A beam energy measurement (2 hrs) and BCM calibrations (2 hrs) will be necessary. We will take optics data at all scattering angles. A 30 minute run on carbon foils for each angle will be sufficient, for a total of 4 hours of optics data. We assume 8 hours for initial checkout, yielding a total of 31 hours for setup, calibration, and background studies.

Configuration changes

Because the ^{3}He cryo-target is now required to run without any other cryo-targets, 8 hours will be needed to perform the target configuration change to ^{2}H and ^{4}He running simultaneously.

Taking into account the fact that the left and the right HRS will be running in parallel and that we will need to repeat all (most) kinematic points with ^{4}He (^{2}H), we require 16 hours for repeating twice the 8 kinematic changes (angle and HRS momentum), and about 8 hours for 46 target changes, assuming 10 min. each. This yields a total of 32 hours for configuration changes.

V. EXPERIMENTS WITH SIMILAR PHYSICS GOALS

Section II provided a detailed comparison to the previous measurements of SRCs. The proposal is complementary to two-nucleon knockout measurements, such as the completed experiment E01-015 [8] and E07-006, approved by PAC31. The inclusive measurements can be combined with the two-nucleon knockout measurements to better study the relative contributions of 2N- and 3N-SRCs [12], as well providing additional information on the isospin dependence of 2N-SRCs.

The effort in the 12 GeV experiment E12-06-105 is heavily weighted toward very large momentum transfers in an attempt to measure the quark distribution functions in nuclei. It will include measurements of cross sections and ratios for $x > 1$ and will be able to reach higher Q^2 for the 3N-SRC and 4N-SRC regions for several light and heavy target. The measurements proposed here will map out scaling at lower Q^2 for a subset of nuclei (as well as the ^{40,48}Ca targets that are not part of the 12 GeV measurement). The measurements proposed here will allow us to determine the Q^2 and x range needed to have a reliable extraction of 3N-SRC. If scaling is verified for the 3N-SRC region at low Q^2 values, then we can measure the contribution of 3N-SRC for ^{4}He and ^{12}C. The 12 GeV measurement will then provide improved data for the large x values, as well as adding several more nuclei. If the scaling region is not reached, or only reached for the higher Q^2 settings, then the current measurement (and the existing CLAS data) are insufficient to measure the strength of 3N-SRCs, and we will know what Q^2 range is needed for reliable 12 GeV measurement. This proposal will make a first exploration in the 4N-SRC region, and provide importance guidance for the E12-06-105 measurements at $x > 3$.

VI. REQUEST TO THE LABORATORY

We are requesting 289 hours (12 days) of beam time: 226 hours for the main data taking, 32 hours for configuration changes, and 31 hours for calibration, checkout, and background runs, all assuming 100% running efficiency. We will need the 20cm ^{2}H, ^{3}He and ^{4}He cryo-targets, and empty cell, the multi-foil optics targets, and three solid targets: 2% RL ^{12}C, 4% RL ^{40}Ca, and 4% RL ^{48}Ca, to achieve our physics goal. We run with the two HRS spectrometers taking data independently using standard dectector packages, and except for the calcium targets, the experiment requires nothing new, and no special equipment or setup.

We request a beam energy of 3.6 GeV, but have flexibility in the exact energy. Slightly lower beam energies would require slightly larger angles to reach the same Q^2, increasing the needed time slightly. Somewhat higher beam energies will allow us to go to slightly smaller angles for the left arm, decreasing the time needed at each Q^2 point, but would make it impossible to take some of the lower Q^2 data in the right arm, due to the limit on the maximum momentum. So we would have to focus the right arm on the highest Q^2 data, and take some of the right arm settings in the left arm, allowing us to complete the measurement with little or no increase in beamtime.

VII. SUMMARY

The proposed experiment will provide precise measurements of a_2 and a_3 for ^{4}He, ^{12}C, ^{40}Ca, ^{48}Ca. The calcium-isotope measurement will be the first in this kinematic region. Using isotopes, we will be able to study the isospin dependence of the 2N-SRCs in inclusive scattering to complement the two-nucleon knockout measurements. This experiment will be the first measurement of the isospin dependence of 3N-SRC, and a first exploration of the ratios above $x = 3$.

This is a high impact measurement testing the scaling assumptions made in the CLAS analysis of 3N-SRC, and making a factor of 2 improvement on both the direct experimental measurement and the extraction of information on three-nucleon correlations. The mapping of the x and Q^2 dependence from our proposed experiment will help in the optimization of already-approved 12 GeV measurements on several few-body and heavy nuclei. It will also be very important in determining the feasibility of similar measurements on ^{3}H and ^{3}He at 12 GeV.

The experiment requests 12 days of beam time, including calibration, overhead, and background measurements, and uses only the HRS spectrometers with standard detector configurations.

---

[1] L. L. Frankfurt and M. I. Strikman, Nucl. Phys. **B181**, 22 (1981).
[2] L. L. Frankfurt and M. I. Strikman, Phys. Rept. **160**, 235 (1988).
[3] C. C. degli Atti and S. Simula, Phys. Lett. B **325**, 276 (1994).
[4] L. L. Frankfurt, M. I. Strikman, D. B. Day, and M. Sargsian, Phys. Rev. C **48**, 2451 (1993).
[5] K. S. Egiyan et al. (CLAS), Phys. Rev. C **68**, 014313 (2003).
[6] K. S. Egiyan et al. (CLAS), Phys. Rev. Lett. **96**, 082501 (2006).
[7] W. Bertozzi, E. Piasetzky, J. Watson, S. Wood, et al., Jefferson Lab experiment E01-015.
[8] R. Shneor et al. (Jefferson Lab Hall A), Phys. Rev. Lett. **99**, 072501 (2007).
[9] K. Egiyan et al., cLAS-NOTE 2005-004, www1.jlab.org/ul/Physics/Hall-B/clas.
[10] M. M. Sargsian, private communication.
[11] M. I. Strikman, private communication.
[12] E. Piasetzky, M. Sargsian, L. Frankfurt, M. Strikman, and J. W. Watson, Phys. Rev. Lett. **97**, 162504 (2006).
[13] J. L. S. Aclander et al., Phys. Lett. **B453**, 211 (1999).
[14] A. Tang et al., Phys. Rev. Lett. **90**, 042301 (2003).
[15] E. Piasetzky, private communication.
[16] R. Schiavilla, R. B. Wiringa, S. C. Pieper, and J. Carlson, Phys. Rev. Lett. **98**, 132501 (2007).
[17] S. C. Pieper and R. B. Wiringa, Ann. Rev. Nucl. Part. Sci. **51**, 53 (2001), nucl-th/0103005.

[18] B. Wiringa, private communication.
[19] G. Petratos, J. Gomez, R. Holt, R. D. Ransome, et al., Jefferson Lab proposal E06-12-118 (conditionally approved).
[20] T. Frick, H. Muther, A. Rios, A. Polls, and A. Ramos, Phys. Rev. **C71**, 014313 (2005).
[21] D. Meekins, private communication.
[22] N. Fomin, Ph.D. thesis, University of Virginia (in preparation).
[23] J. Arrington et al., Phys. Rev. Lett. **82**, 2056 (1999).
[24] P. Solvignon, Ph.D. thesis, Temple University (2006).
[25] J. Alcorn et al., Nucl. Inst. & Meth. **A522**, 294 (2004).
[26] O. Benhar, D. Day, and I. Sick (2006), nucl-ex/0603029.
[27] Z. E. Meziani et al., Phys. Rev. Lett. **69**, 41 (1992).
[28] J. Seely, Ph.D. thesis, Massachusetts Institute of Technology (2006).